analytical chemistry

Article

pubs.acs.org/ac

Enzyme-Modified Carbon-Fiber Microelectrode for the Quantification of Dynamic Fluctuations of Nonelectroactive Analytes Using Fast-Scan Cyclic Voltammetry

Leyda Z. Lugo-Morales,[†] Philip L. Loziuk,[†] Amanda K. Corder,[†] J. Vincent Toups,[†] James G. Roberts,[†] Katherine A. McCaffrey,[‡] and Leslie A. Sombers*[,†]

[†]Department of Chemistry and [‡]Department of Biology, North Carolina State University, Raleigh, North Carolina 27695, United States

Supporting Information

ABSTRACT: Neurotransmission occurs on a millisecond time scale, but conventional methods for monitoring nonelectroactive neurochemicals are limited by slow sampling rates. Despite a significant global market, a sensor capable of measuring the dynamics of rapidly fluctuating, nonelectroactive molecules at a single recording site with high sensitivity, electrochemical selectivity, and a subsecond response time is still lacking. To address this need, we have enabled the real-time detection of dynamic glucose fluctuations in live brain tissue using background-subtracted, fast-scan cyclic voltammetry. The novel microbiosensor consists of a simple carbon fiber surface modified with an electrodeposited chitosan hydrogel encapsulating glucose oxidase. The selectivity afforded by voltammetry enables quantitative and qualitative measurements of enzymatically generated H_2O_2 without the need for additional strategies to eliminate interfering agents. The microbiosensors possess a sensitivity and limit of detection for glucose of 19.4 ± 0.2 nA mM^{-1} and 13.1 ± 0.7 μM, respectively. They are stable, even under deviations from physiological normoxic conditions, and show minimal interference from endogenous electroactive substances. Using this approach, we have quantitatively and selectively monitored pharmacologically evoked glucose fluctuations with unprecedented chemical and spatial resolution. Furthermore, this novel biosensing strategy is widely applicable to the immobilization of any H_2O_2 producing enzyme, enabling rapid monitoring of many nonelectroactive enzyme substrates.

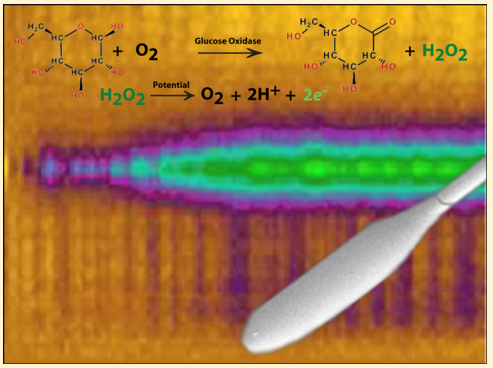

Neuroscientists depend on reliable methods for neurochemical monitoring because brain function is governed by subsecond neurotransmission events. Electrochemical techniques provide instantaneous information, making them especially useful for monitoring rapid chemical changes in vivo. Advances in voltammetry have considerably expanded the scope of neurochemical studies by enabling quantification of fluctuations of molecules such as dopamine (DA), a neurotransmitter that is important in movement and reward processes.[1] The principle by which fast-scan cyclic voltammetry (FSCV) operates allows DA to be distinguished from interfering agents in the brain at bare carbon-fiber electrodes, not because of an interference-excluding membrane, but because the analyte has electrochemistry that can be differentiated from the electrochemistry of the interfering agents.[2] However, the voltammetric approach is limited to electroactive molecules, and information associated with rapid fluctuations of countless nonelectroactive molecules in the brain, including glucose, remains obscure. This is largely due to limitations associated with the traditional use of enzyme-modified electrodes.

Clark and Lyons developed the first enzyme-modified electrode in 1962, which detected glucose by the amperometric detection of electroactive hydrogen peroxide (H_2O_2) produced by glucose oxidase (GOx) on the electrode surface.[3] Since then, biosensors that generate H_2O_2 to report on the presence of nonelectroactive analytes have become one of the most active and clinically important research areas.[4] As reviewed by Wilson et al., many useful studies have been carried out using enzyme-modified electrodes.[5−7] The overwhelming majority of enzyme-modified electrodes are constructed of platinum, because this material provides an electro-catalytic surface for the kinetically slow electro-oxidation of H_2O_2.[4,8] However, metal electrodes can exhibit unstable electrochemical backgrounds, particularly in the first 4−6 h after implantation in tissue, due to nonspecific adsorption of biological molecules to the electrode surface.[1] Furthermore, they are traditionally coupled with constant-potential amperometry, a technique that does not offer electrochemical selectivity, because all oxidizable species that are present contribute to the measured current. Thus, these electrodes require multiple polymeric coatings, or the incorporation of additional enzymes, to reduce interferences. These membranes also serve to optimize a linear response and

Received: June 26, 2013
Accepted: August 6, 2013
Published: August 6, 2013

   dx.doi.org/10.1021/ac4017852 | Anal. Chem. 2013, 85, 8780−8786

to minimize dependence on fluctuations of enzyme cosubstrates.[5,9,10] Stability and selectivity are dependent on coating integrity, and performance is slowed due to increased diffusion coefficients for analytes traveling through multiple coatings.[11] It is also common to use a second, nonenzyme-modified recording site to verify the signal in a self-referencing spatial subtraction paradigm.[12,13] This approach provides meaningful information on larger chemical changes but can introduce inaccuracy or even report negative concentrations, because each electrode differs in background current and substrate sensitivity. Furthermore, recent studies have revealed an unanticipated and significant chemical heterogeneity at brain recording sites as little as 75 μm apart, and chemical dynamics vary on a subsecond time scale.[14] Thus, spatial and temporal averaging also compromises accuracy. Additionally, electrical crosstalk can occur between the enzyme-coated electrode and the null electrode, precluding their simultaneous use in vivo. In this case, recordings are made sequentially at each electrode, sometimes over multiple days, and are then subtracted to generate the analytical signal.[12,15]

Brain glucose metabolism is dynamically regulated and dependent on brain region, as well as physiological and pathological conditions.[16−18] At any moment, extracellular brain glucose concentration is defined by the amount of glucose transported to a site, less the amount locally metabolized. However, studies aimed at elucidating these dynamics and the complex metabolic coupling between neurons and astrocytes have been limited by the lack of a direct method for probing glucose dynamics in intact brain tissue with subsecond temporal and precise spatial resolution. As a result, significant gaps exist in our understanding of how impaired glucose utilization contributes to the onset of many conditions including stroke, Alzheimer's disease, Parkinson's disease, Huntington's disease, cancer, and schizophrenia.[19−22] To address these important gaps, we have developed a genuinely new, fast-scan voltammetric detection scheme for H_2O_2[23] and we use it herein at novel enzyme-modified carbon-fiber microelectrodes to overcome the limitations typically associated with enzyme-modified electrodes. With this approach, electroactive analytes can be monitored at the single recording site during the detection of glucose dynamics in real-time. If the additional analytes (or interfering agents) are electroactive and have electrochemistry that is different from that of H_2O_2, then chemical resolution is possible. Using this strategy, we report the first quantitative characterization of brain glucose events with subsecond temporal resolution.

EXPERIMENTAL SECTION

Chemicals. All chemicals were purchased from Sigma-Aldrich (St. Louis, MO), unless otherwise noted, and used as received. Phosphate buffer saline (10 mM PBS, pH 7.4, containing 138 mM NaCl and 2.7 mM KCl) at pH 7.4 was filtered using a 0.2 μm nylon vacuum filtration system (VWR International, West Chester, PA). O_2 or N_2 gas was used to increase or decrease the concentration of dissolved O_2, respectively. O_2 concentration was quantified using a dissolved O_2 meter (Fisher Scientific Accumet BOD probe). Calibration of microelectrodes was performed in a Tris buffer solution (15 mM Trizma HCl, 3.25 mM KCl, 1.2 mM $CaCl_2$, 1.2 $MgCl_2$, 2.0 mM Na_2SO_4, 1.25 mM NaH_2PO_4, and 145 mM NaCl) at pH 7.4. β-D-Glucose and GOx from *Aspergillus niger* were acquired from VWR International (West Chester, PA). The chitosan was from shrimp shells and had a deacetylation percentage of ≥75% and an approximate molecular weight of 190 000−375 000 Da (practical grade). Glucose stock solution was prepared and allowed to undergo mutarotation for at least 24 h at room temperature. All aqueous solutions were made using doubly distilled deionized water (Millipore Milli-Q, Billerica, MA).

Microelectrode Fabrication. Cylindrically shaped carbon-fiber microelectrodes were fabricated as previously described.[23] Briefly, a single T-650 carbon fiber (7 μm diameter, Cytec Industries, West Patterson, NJ) was aspirated into a borosilicate glass capillary (1.0 mm × 0.5 mm, A-M Systems, Carlsburg, WA). A micropipet puller (Narishige, Tokyo, Japan) was used to taper the glass and form two sealed microelectrodes. The exposed length of the carbon fiber was cut to approximately 100 μm. The microelectrodes were electrochemically conditioned for 15 min using a triangular waveform that ranged from −0.4 to +1.4 V (vs Ag/AgCl), applied at 400 V/s at a frequency of 60 Hz, and then applied at 10 Hz for an additional 5 min.

Microbiosensor Fabrication. Conditioned carbon-fiber microelectrodes were lowered into a solution of 30 mg of GOx (6 mg/mL GOx, pH 5.0, specific activity: 116 U/mg at 37 °C) dissolved in 5 mL of 1% chitosan (aqueous). A DC power supply was used to apply −3.0 V (vs Ag/AgCl), a potential sufficient to reduce protons to H_2 gas. Thus, a pH gradient was generated at the microelectrode surface, and chitosan was deprotonated and electrodeposited as a film on the microelectrode surface, locally encapsulating GOx. Electrodeposition was performed for 30 s followed by visual inspection of the electrode using an optical microscope. If adequate membrane formation did not occur (see Figure 1B), electrodeposition was continued for an additional 30 s. The microbiosensors were stored in PBS overnight at 4 °C. Heat-inactivated sensors were prepared by heating the GOx to 90 °C prior to electrodeposition.

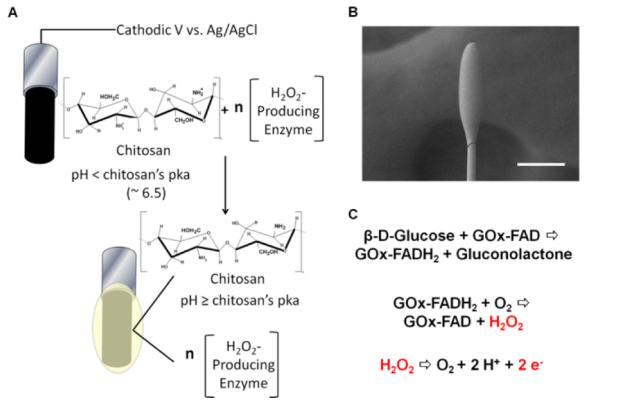

Figure 1. Carbon-fiber microbiosensors. (A) Schematic illustrating the electrodeposition of chitosan. (B) Scanning electron micrograph of a carbon-fiber microelectrode with an electrodeposited chitosan membrane encapsulating GOx. Scale bar = 50 μm (see Experimental Section). (C) GOx catalytic reaction in the presence of β-D-glucose and with O_2 as the cosubstrate.

Electrochemical Data Acquisition. All in vitro data were collected at room temperature in a flow injection apparatus. The microbiosensor was positioned in a custom electrochemical cell using a micromanipulator (World Precision Instruments, Inc., Sarasota, FL). A syringe pump (New Era Pump Systems, Inc., Wantagh, NY) supplied a continuous buffer flow of 0.5 mL/min (unless otherwise indicated). Five second bolus injections of analyte were accomplished with a six-

dx.doi.org/10.1021/ac4017852 | Anal. Chem. 2013, 85, 8780−8786

port HPLC valve mounted on a two-position air actuator controlled by a digital pneumatic solenoid valve (Valco Instruments Co., Inc., Houston, TX). The apparatus was housed within a grounded Faraday cage.

Unless otherwise noted, a triangular voltammetric waveform ranging from +0.1 to +1.4 V (vs Ag/AgCl) was applied at 400 V/s at a collection rate of 10 Hz using a custom instrument built for potential application and current transduction (United World Domination, Mebane, NC). Each potential cycle had a duration of 6.5 ms, and the microelectrode was held at +0.1 V between scans (Figure 2A). TH-1 software (ESA, Chelmsford, MA) was used for waveform output with a DAC/ADC card (NI 6251 M). A second card (NI 6711) was used for triggering the DACs and ADCs and for synchronization of the electrochemical experiment with flow injection. A nonlinear color scale was used to represent the current.[24] Analog filtering was performed using a 4-pole Bessel filter, 2.5 kHz. Signal processing (background subtraction, signal averaging, and digital filtering) was software controlled. Background subtraction was done for each individual 30 s data file.

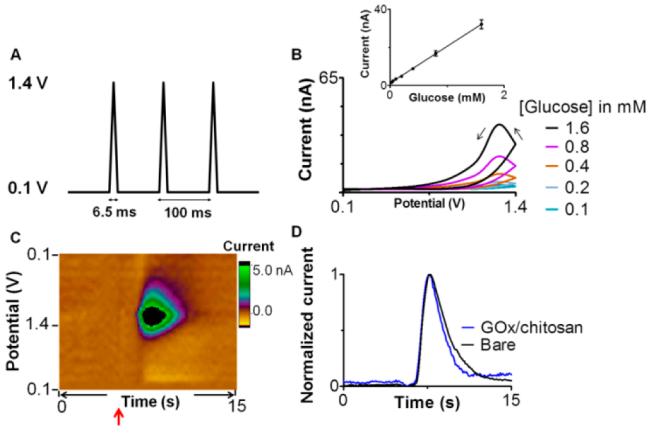

Figure 2. Voltammetric detection of glucose at GOx/chitosan-modified microelectrodes. (A) A triangular potential waveform is applied to the electrode and ramped from +0.1 to +1.4 V and back at a scan rate of 400 V/s and a frequency of 10 Hz. (B) Background-subtracted voltammograms for H_2O_2 enzymatically generated in response to glucose. Inset, linear response to physiological glucose concentrations (n = 5). Error bars, ± SEM. (C) Representative color plot composed of voltammograms obtained in response to glucose (arrow) plotted with respect to the applied potential (V, y-axis) and collection time (s, x-axis). Each successive cyclic voltammogram is plotted with the current (nA) shown in false color. (D) The normalized average response to a supra-physiological concentration of H_2O_2 at the microbiosensors (blue) was not delayed when compared to the response at bare microelectrodes (black), demonstrating that the chitosan membrane did not slow the response time (n = 3, two-tailed paired t test, t = 0.5, p = 0.6667).

For amperometric experiments, a holding potential of +1 V was applied and data was collected at a frequency of 3 kHz using an Axopatch 200B Patch Clamp Amplifier (Molecular Devices, Sunnyvale, CA) and a low-noise headstage (model CV-203BU). The output was filtered at 1 kHz using a low-pass Bessel filter (80 dB/Decade). Data was displayed using software written in house using LabView (version 9.0.0, National Instruments, Austin, TX) and MATLAB (version R2009b, The MathWorks, Natick, MA) and stored to the computer with no subsequent filtering.

In Vivo Experiments. All animal procedures followed the North Carolina State University Institutional Animal Care and Use Committee (IACUC) guidelines. Male Sprague-Dawley rats (n = 5, 290 - 320 g, Charles River, Wilmington, MA) with jugular vein catheters were anesthetized with urethane (4.1−4.8 g/kg intraperitoneally) and placed in a stereotaxic frame (David Kopf Instruments, Tujunga, CA). A Ag/AgCl reference electrode was placed in the forebrain, and a GOx/chitosan-modified microelectrode was placed in the caudate putamen (CPU) (+1.2 mm anteroposterior (AP), +3.6 mm mediolateral (ML), and −4.5 to −6.0 mm dorsoventral (DV), relative to bregma). The animal's body temperature was maintained at 37 °C by a heating pad (Braintree Scientific, Braintree, MA). Electrochemical data was collected before and after a 0.6 mL infusion of saline and a 0.3−1.0 mL injection of 30−50% glucose (Hospira Inc., Lake Forest, IL) immediately followed by 0.3 mL of saline. In some animals (n = 3), a heat-inactivated microbiosensor was also positioned in the contralateral CPU (+1.2 mm AP, −3.6 mm ML, −4.5 to −6.0 mm DV). Potential was applied to, and current sampled from, both enzyme-modified microelectrodes simultaneously using a multiple-channel universal electrochemistry instrument (UEI, UNC-Chapel Hill electronics design facility, Chapel Hill, NC). Both carbon-fiber microelectrodes were referenced against the same Ag/AgCl reference electrode.

Variable Pressure Scanning Electron Microscopy. Microbiosensors were imaged in a Hitachi S-3200 variable pressure scanning electron microscope (150 Pa). A metallized coating on the electrodes was not required. The accelerating voltage used was 5 kV. A 4Pi EDS/Digital Imaging system was used for digital image acquisition.

Microelectrode Calibration. Freshly prepared GOx/chitosan-modified microelectrodes were precalibrated in a flow injection apparatus at room temperature to identify those with an experimental limit of detection of at least 0.1 mM glucose, which were then selected for experiments. Postcalibration was done for ascorbic acid (AA), DA, glucose, and basic pH shifts using physiological concentrations of these analytes.

Data Analysis and Statistics. Analytes were resolved with principal component regression (PCR) using MATLAB (MathWorks, Natick, MA).[2,25] Limit of detection was defined as three times the noise. All values are given as the mean ± standard error of the mean (SEM). Two-tailed paired t test, two-tailed unpaired t test, and one-way analysis of variance (ANOVA) with Bonferroni's multiple comparisons posthoc analyses were used to determine statistical differences using GraphPad Prism 5 (GraphPad Software, Inc., La Jolla, CA). For the comparison of electrode sensitivities, a model with random effects was performed using SAS Proc Mixed (SAS Institute Inc., SAS Campus Drive, Cary, NC). In all cases, significance was designated as $p < 0.05$.

Histology. Details provided in Supporting Information.

RESULTS AND DISCUSSION

Voltammetric Microbiosensor Fabrication. Chitosan is a natural polysaccharide derived from chitin, which has a high affinity for proteins and has been used extensively for enzyme immobilization.[26−29] Minimally invasive carbon-fiber microelectrodes (~7 μm in diameter) were modified with a nontoxic chitosan matrix using electrodeposition in order to confine GOx in close proximity to the electrode surface. Figure 1A depicts the electrodeposition process. The solubility of chitosan can be manipulated by application of a cathodic potential,

dx.doi.org/10.1021/ac4017852 | Anal. Chem. 2013, 85, 8780−8786

which locally shifts the pH of the solution. When the pH exceeds the pK_a of chitosan (>∼6.5), chitosan polymerizes into a hydrogel at the electrode surface. Figure 1B shows a scanning electron micrograph of a modified carbon-fiber microelectrode with an approximate diameter of 20 μm and an approximate length of 100 μm. The enzymatic reaction is depicted in Figure 1C. The oxidized form of the GOx cofactor, flavin adenine dinucleotide (FAD), is reduced as glucose is oxidized to gluconolactone, generating H_2O_2. The electrochemical oxidation of H_2O_2 generates O_2, 2 protons and 2 electrons, and is measured as a change in current.

In FSCV, a dynamic potential is rapidly applied to a carbon-fiber microelectrode (Figure 2A), and current is recorded as a function of potential. The characteristic voltammogram allows analyte identification. Our simple approach provides unprecedented temporal and spatial resolution because a complete voltammetric signature composed of 1000 data points is acquired every 100 ms at a single 100 μm recording site without requiring spatial subtraction schemes, the addition of redox mediators, or chemically selective coatings.

In Vitro Characterization. The novel microbiosensors were characterized in a flow injection apparatus, in which a bolus of glucose was reproducibly introduced to the electrode surface. The background-subtracted voltammograms show a single peak at ∼+1.2 V (Figure 2B), indicative of the voltammetric signature for H_2O_2 when using this approach.[23] Physiological glucose concentrations generated a linear response (n = 5, r^2 = 0.999, p < 0.0001; Figure 2B) with a limit of detection of 13.1 ± 0.7 μM and sensitivity of 19.4 ± 0.2 nA/mM glucose or 8.67 × 10^5 nA·mM^{-1}·cm^{-2} (in terms of current density). A representative color plot containing 150 background-subtracted cyclic voltammograms recorded over 15 s is shown in Figure 2C. The ordinate is the applied potential; the abscissa is time, and the current (nA) is depicted in false color. The signal observed is due to the oxidation of H_2O_2 produced in response to a glucose injection (arrow in Figure 2C).

The GOx/chitosan hydrogel did not slow the detection performance, as the time-response to a supra-physiological concentration of H_2O_2 (50 μM) was not significantly different between enzyme-modified and bare microelectrodes (0.73 ± 0.09 and 0.77 ± 0.03 s, respectively; n = 3, t = 0.5, p = 0.6667; Figure 2D). Current vs time traces for repeated injections of 1.6 mM glucose were used to determine the average response time for the carbon-fiber microbiosensors employed with FSCV, based on the time it took a current peak signal to rise from 10% to 90% of its maximum value. This was measured to be 0.90 ± 0.06 s (n = 3). As a point of comparison, amperometric studies using comercially produced GOx/polymer-coated Pt−Ir microelectrodes report response times of ∼4−30 s.[12,15,30,31] However, it should be noted that response times are dependent on many different experimental parameters, such as concentration of the generated H_2O_2, geometry and area of the electrode, restrictions to mass transfer, and the nature of the convective flow used for signal characterization. The microbiosensors presented herein have a chitosan thickness estimated to be 5.7 ± 0.2 μm (n = 3) using a previously described model[32] (see Figure S-1 in Supporting Information).

The kinetic parameters of the microbiosensor were determined by fitting an extended calibration plot to the electrochemical version of the Michaelis−Menten equation (see Supporting Information). Under enzyme kinetic control, a plateau current is observed when plotting concentrations of substrate beyond the dynamic linear range (Figure 3). The K_M^{app} value serves as a measure of the stability of the enzyme−substrate complex, being equal to the rate of breakdown of this complex divided by its rate of formation, and i_{max} represents the current measured from the oxidation of enzymatically generated H_2O_2 under substrate saturation conditions.[33] The i_{max} and K_M^{app} values were 85.7 ± 9.6 nA and 3.0 ± 0.6 mM glucose, respectively (n = 5, r^2 = 0.99, P = 0.3714). These are comparable to values published for conventional amperometric electrodes employing chitosan for GOx immobilization,[34,35] indicating high glucose affinity and high enzymatic activity for its conversion.

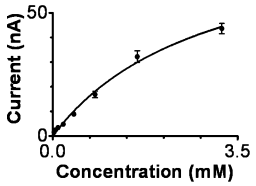

Figure 3. Immobilized enzyme kinetics. Michaelis−Menten kinetic nonlinear fit for the response of the microbiosensors to glucose concentrations ranging from 0.025 to 3.2 mM (n = 5, r^2 = 0.99, p = 0.3714). The K_M^{app} and i_{max} values are 3.0 ± 0.6 mM and 85.7 ± 9.6 nA, respectively.

Stability was verified by introducing a bolus of glucose to the microelectrode every 10 min over a 4 h time period (Figure 4A). There was no significant difference between the initial signal and that collected at subsequent times (n = 3, F = 0.3155, p = 0.9984). The enzymatic consumption of glucose requires O_2 as the cosubstrate, which fluctuates in a living system.[36] Mirobiosensor performance was not significantly affected by O_2 fluctuations that exceeded the physiological range, despite the

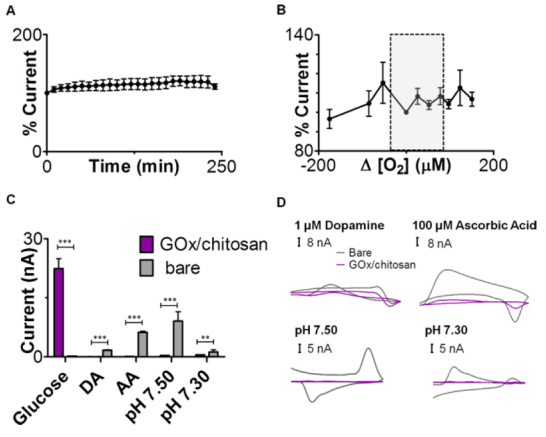

Figure 4. In vitro characterization. Electrode response was stable (A) over 4 h (F = 0.3155, P = 0.9984) and (B) in a supra-physiological range of O_2 concentrations (n = 3, one-way ANOVA with Bonferroni's multiple comparisons post test, F = 0.9430, P = 0.5114). The approximate physiological range of O_2 concentration is depicted in gray. (C) Averaged response to glucose (1.6 mM), dopamine (500 nM), ascorbic acid (50 μM), and pH shifts at enzyme-modified (purple) and bare (gray) microelectrodes. No significant interference was observed (n = 3, two-tailed paired t test, t_{DA} = 9.363, t_{AA} = 24.21, $t_{pH7.50}$ = 3.795, $t_{pH7.30}$ = 9.995, ***p < 0.0001, **p = 0.0016). Glucose is not detected at bare electrodes due to its nonelectroactive nature. (D) Averaged cyclic voltammograms for DA, AA, and pH at bare (gray) and GOx/chitosan-modified (purple) microelectrodes (n = 3).

dx.doi.org/10.1021/ac4017852 | Anal. Chem. 2013, 85, 8780−8786

lack of an outer diffusional barrier to limit glucose flux (n = 3, F = 0.9430, p = 0.5114; Figure 4B).

Selectivity was assessed by detecting glucose (1.6 mM) and the common interfering agents DA (500 nM and 1 μM), AA (50 μM and 100 μM), and pH at bare and enzyme-modified microelectrodes (Figure 5C,D). The enzyme-modified electrodes were insensitive to the physiological concentrations of AA and DA (n = 3; t_{DA} = 9.363, t_{AA} = 24.31, ***p < 0.0001), likely because the few protonated amine functionalities on chitosan at physiological pH[37] can repel and/or retain charged species,[28] limiting their diffusion to the microelectrode surface. It was important to investigate pH, as local pH fluctuations correlate with brain energy metabolism in which glucose is a key player.[38] Figure 4C,D demonstrates that 0.1 unit pH fluctuations are not detectable at the enzyme-modified microelectrodes (n = 3; $t_{pH7.30}$ = 9.995, ***p < 0.0001 and $t_{pH7.50}$ = 3.795, **p = 0.0016 for acidic and basic pH shifts, respectively). Finally, H_2O_2 is endogenously generated and thus is itself a potential interfering agent, though it is often overlooked. There is little consensus on the range of endogenous H_2O_2 concentrations in the brain, largely due to the lack of sensitive and specific methodologies for the quantitative and dynamic assessment of H_2O_2 in living tissue.[39] Bare electrodes were significantly (52.7%) more sensitive to H_2O_2 than enzyme-modified electrodes ($t_{df=6.82}$ = 3.76, p = 0.0074). A supra-physiological H_2O_2 concentration (50 μM) produced ~13 nA of current at bare electrode but only ~6 nA at GOx/chitosan-modified microelectrodes. In comparison, 300 μM glucose produced ~6 nA of current at enzyme-modified microelectrodes. This concentration of glucose is at the low end of the physiological range.

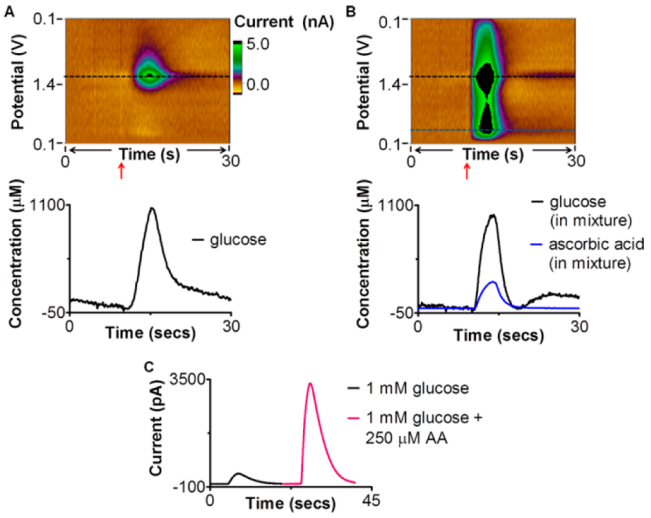

Figure 5. Comparison of FSCV and amperometry. (A, B) Voltammetric data. Representative color plots (top panels) and respective analyte concentration vs time traces (bottom panel) collected at a GOx/chitosan-modified carbon-fiber microelectrode in response to a bolus injection (arrow) of (A) 1 mM glucose (black) or (B) a sample containing 1 mM glucose (black) in the presence of AA (250 μM, blue). Concentration vs time traces for both analytes were extracted from the data using principal component regression. Glucose and ascorbic acid were readily distinguished and simultaneously quantified. (C) Amperometric data. When the same solutions were interrogated with the microbiosensor held at a constant potential of +1.0 V, the two analytes could not be distinguished and the current from the oxidation of AA was evident in the signal (pink).

Comparison with Amperometry. The advantages of the voltammetric approach are readily evident when comparing the performance of the microbiosensors using FSCV and conventional amperometry. Figure 5 compares data collected in response to a physiological concentration of glucose (1 mM) and a mixture of 1 mM glucose and AA (250 μM). Using FSCV (Figure 5A,B), the glucose sample generated H_2O_2 at the enzyme-modified electrode surface and the oxidation of this electroactive product was collected as current at ~+1.2 V (Figure 5A, top). The concentration vs time trace extracted from the data is also presented (bottom). In contrast, the single injection of the mixture generated anodic current at two distinct potentials, as shown in Figure 5B (top). The currents due to the oxidation of H_2O_2 (~+1.2 V) and AA (~+0.4 V) are simultaneously quantifiable. FSCV is a multivariate technique whereby the shape of the cyclic voltammogram can serve as an identifier for the measured analyte. Thus, PCR was used to extract concentration vs time traces for both analytes (Figure 5B, bottom). AA does not interfere with the detection of glucose, despite the lack of polymeric membranes to promote chemical selectivity. In contrast, the presence of AA was a problem when using amperometric detection. Figure 5C shows current collected at +1.0 V in response to the same glucose sample (black), followed by the mixture (pink). When responding to the sample containing both glucose and AA, current produced by the oxidation of enzymatically generated H_2O_2 could not be distinguished from that produced by the oxidation of AA. These data demonstrate how the electrochemical selectivity inherent to FSCV enables multiple analytes to be simultaneously detected and quantified at a single enzyme-modified carbon-fiber microelectrode, without requiring polymeric coatings and/or self-referencing schemes to exclude interference signals.

In Vivo Characterization. To demonstrate that the GOx/chitosan biosensors can selectively monitor rapid changes in glucose concentration in vivo, voltammograms were simultaneously collected at a GOx/chitosan-modified electrode implanted in the CPU of one hemisphere and at a heat-inactivated but otherwise identical microbiosensor implanted in the contralateral CPU. Intravenous (i.v.) infusion of glucose (120−300 mg in 0.3−1.0 mL of saline over 30 s) generated a 0.388 ± 0.168 mM increase in striatal glucose detected only on the active microbiosensor (Figure 6A,C). A small intermittent signal was collected on the heat-inactivated microelectrode but at a significantly reduced intensity when compared to the enzymatically active microbiosensor located across the brain ($t_{df=598}$ = 30.27, p < 0.0001). Postcalibration indicated that this heat-inactivated electrode possessed some residual enzymatic activity (Figure 6D); however, we cannot rule out the possibility that the residual signal is due to endogenous H_2O_2 signaling in this brain region.[40] Histological examination of microelectrode placement in select animals confirmed that recordings were made in the dorsal striatum (data not shown), a region previously estimated to contain 0.47 mM glucose using microdialysis in awake rats.[41]

Glucose transporter type 1 (GLUT1) is the main glucose carrier at the blood−brain barrier and, under normal conditions, it does not limit the rate of brain glucose consumption,[20,42] which is precisely controlled to maintain optimal learning, memory, and cognitive function.[20,43,44] However, the lack of a direct approach to measure real-time changes in brain glucose concentration with precise spatial and subsecond temporal resolution has limited studies investigating

dx.doi.org/10.1021/ac4017852 | Anal. Chem. 2013, 85, 8780−8786

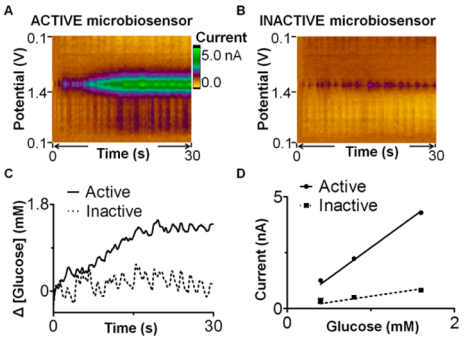

Figure 6. Dual-probe measurements. Representative voltammetric data collected simultaneously at an active (A) and at a heat-inactivated (B) microbiosensor in response to an i.v. glucose infusion. (C) Representative glucose concentration traces extracted from the voltammetric data. (D) Postcalibration demonstrated that the active electrode was significantly more sensitive to glucose than the inactivated electrode, which demonstrated some residual enzymatic activity (F = 5394.07, p = 0.00019). Error bars, ± SEM of three replicate injections of each glucose concentration.

the mechanisms linking ATP production (by way of glycolysis or oxidative phosphorylation) to neural activity. The canonical model involving the astrocyte-neuron lactate shuttle proposed by Pellerin and Magistretti[45] is hotly debated. Indeed, a recent study carried out on rat brain slices has demonstrated that the majority of the ATP production triggered by increased neuronal activity is produced by oxidative phosphorylation.[46] This calls into question the simplest version of the astrocyte-neuron lactate shuttle hypothesis, in which neuronal activity initially triggers the generation of ATP by glycolysis in astrocytes, which then release lactate to rapidly power neuronal oxidative phosphorylation. Similar studies carried out in intact systems, with subsecond temporal resolution, are necessary to clarify this issue. Other recent studies have indicated that extracellular glucose concentration changes in a manner that is both region and activity dependent;[47−49] however, these studies were sampled on a slower time scale and utilized larger probes, thus both spatially and temporally averaging site-specific differences. One recent study in awake animals that utilized the differential between amperometric current collected using GOx-modified and, on a separate day, enzyme-null commercial electrodes reported that i.v. infusion of a lower dose of glucose (15 mg) induced an ∼100 μM increase in glucose concentration in the nucleus accumbens (NAc) and ∼65 μM increase in the substantia nigra (SN) of awake rats.[12]

CONCLUSIONS

Our simple and reliable approach has enabled the first subsecond characterization of dynamic glucose fluctuations in intact brain tissue at micrometer-scale single recording sites, because the selectivity afforded by voltammetric detection precludes the requirement for signal subtraction across enzyme and enzyme-null electrodes, or the addition of chemically selective coatings that limit mass transfer to the recording site, slowing detection. We have demonstrated exquisite sensitivity because the enzyme is immobilized on the electrode surface by way of electrodeposition in chitosan, an approach that produces minimal disruption of three-dimensional structure of the protein and thus preserves robust enzymatic activity. Furthermore, the chitosan matrix is nontoxic[37] and broadly applicable to the encapsulation of any H_2O_2-producing enzyme. These novel microbiosensors are stable over the time course of a daily experimental session and over a broad range of oxygen concentrations spanning normoxic conditions. Due to the critical role of glycolysis in the maintenance of high brain function, research into the relationship between glucose concentration and neural function should be a high priority. This method will enable countless new experiments that require the detection of real-time glucose dynamics in live tissue and will fulfill a critical need in neuroscience.

ASSOCIATED CONTENT

Supporting Information

Experimental details for the determination of chitosan thickness, characterization of Michaelis−Menten kinetics, and histology; a figure for the determination of chitosan thickness. This material is available free of charge via the Internet at http://pubs.acs.org.

AUTHOR INFORMATION

Corresponding Author

*E-mail: lasomber@ncsu.edu.

Notes

The authors declare no competing financial interest.

ACKNOWLEDGMENTS

We thank Lingjiao Qi and Marina Spanos for critique of drafts of this manuscript; Parastoo Hashemi and Q. David Walker for thoughtful discussion; Consuelo Arellano, Eric Stone, and Pedro Torres for statistical advice; Charles Mooney for equipment and technical assistance. The initial sensor design was supported by the U.S. National Institutes of Health (R03-DA027969 to L.A.S.). Optimization of the probe and its application to glucose monitoring in tissue was supported by the National Science Foundation (CAREER CHE 1151264 to L.A.S.). Leyda Z. Lugo-Morales was supported by the National Science Foundation through a N.C. Louis Stokes Alliance for Minority Participation Fellowship and was also supported by the U.S. Department Of Education Graduate Assistance In Areas Of National Need (GAANN) Fellowship.

REFERENCES

(1) Robinson, D. L.; Hermans, A.; Seipel, A. T.; Wightman, R. M. *Chem. Rev.* **2008**, *108*, 2554−2584.
(2) Heien, M. L.; Johnson, M. A.; Wightman, R. M. *Anal. Chem.* **2004**, *76*, 5697−5704.
(3) Clark, L. C.; Lyons, C. *Ann. N.Y. Acad. Sci.* **1962**, *102*, 29−45.
(4) Wilson, G. S.; Johnson, M. A. *Chem. Rev.* **2008**, *108*, 2462−2481.
(5) Chen, X.; Matsumoto, N.; Hu, Y.; Wilson, G. S. *Anal. Chem.* **2002**, *74*, 368−372.
(6) Cui, J.; Kulagina, N. V.; Michael, A. C. *J. Neurosci. Methods* **2001**, *104*, 183−189.
(7) Wilson, G. S.; Johnson, M. A. *Chem. Rev.* **2008**, *108*, 2462−2481.
(8) Hall, S. B.; Khudaish, E. A.; Hart, A. L. *Electrochim. Acta* **1998**, *43*, 2015−2024.
(9) Chen, X.; Hu, Y.; Wilson, G. S. *Biosens. Bioelectron.* **2002**, *17*, 1005−1013.
(10) Hu, Y.; Wilson, G. S. *J. Neurochem.* **1997**, *68*, 1745−1752.
(11) Bard, A. J.; Faulker, L. R. *Electrochemical Methods*, 2nd ed.; Wiley: New York, 2001.
(12) Kiyatkin, E. A.; Lenoir, M. *J. Neurophysiol.* **2012**, *108*, 1669−1684.
(13) Hascup, K. N.; Rutherford, E. C.; Quintero, J. E.; Day, B. K.; Nickell, J. R.; Pomerleau, F.; Huettl, P.; Burmeister, J. J.; Gerhardt, G.

A. In *Electrochemical Methods for Neuroscience*; Michael, A. C., Borland, L. M., Eds.; CRC Press: Boca Raton, 2007; pp 407−450.
(14) Wightman, R. M.; Heien, M. L.; Wassum, K. M.; Sombers, L. A.; Aragona, B. J.; Khan, A. S.; Ariansen, J. L.; Cheer, J. F.; Phillips, P. E.; Carelli, R. M. *Eur. J. Neurosci.* **2007**, *26*, 2046−2054.
(15) Kiyatkin, E. A.; Wakabayashi, K. T.; Lenoir, M. *ACS Chem. Neurosci.* **2013**, *4*, 652−665.
(16) Raichle, M. E. *J. Neurosci.* **2003**, *23*, 3959−3962.
(17) Reiman, E. M.; Caselli, R. J.; Yun, L. S.; Chen, K.; Bandy, D.; Minoshima, S.; Thibodeau, S. N.; Osborne, D. *N. Engl. J. Med.* **1996**, *334*, 752−758.
(18) Shulman, G. L.; Corbetta, M.; Buckner, R. L.; Raichle, M. E.; Fiez, J. A.; Miezin, F. M.; Petersen, S. E. *Cereb. Cortex* **1997**, *7*, 193−206.
(19) Belanger, M.; Allaman, I.; Magistretti, P. J. *Cell Metab.* **2011**, *14*, 724−738.
(20) Dwyer, D. S., Ed. *Glucose Metabolism in the Brain*; Elsevier Science (USA): San Diego, 2002.
(21) Gatenby, R. A.; Gillies, R. J. *Nat. Rev. Cancer* **2004**, *4*, 891−899.
(22) Lavoie, S.; Allaman, I.; Petit, J. M.; Do, K. Q.; Magistretti, P. J. *PLoS One* **2011**, *6*, No. e22875.
(23) Sanford, A. L.; Morton, S. W.; Whitehouse, K. L.; Oara, H. M.; Lugo-Morales, L. Z.; Roberts, J. G.; Sombers, L. A. *Anal. Chem.* **2010**, *82*, 5205−5210.
(24) Michael, D. J.; Joseph, J. D.; Kilpatrick, M. R.; Travis, E. R.; Wightman, R. M. *Anal. Chem.* **1999**, *71*, 3941−3947.
(25) Keithley, R. B.; Carelli, R. M.; Wightman, R. M. *Anal. Chem.* **2010**, *82*, 5541−5551.
(26) Tajima, S.; Hashiba, M.; Suzuki, T.; Akanuma, H.; Yabuuchi, M. *Biomed. Chromatogr.* **1993**, *7*, 41−44.
(27) Muzzarelli, R. A.; Barontini, G.; Rocchetti, R. *Biotechnol. Bioeng.* **1976**, *18*, 1445−1454.
(28) Zangmeister, R. A.; Park, J. J.; Rubloff, G. W.; Tarlov, M. J. *Electrochim. Acta* **2006**, *51*, 5324−5333.
(29) Krajewska, B. *Enzyme Microb. Technol.* **2004**, *35*, 126−139.
(30) Gifford, R.; Batchelor, M. M.; Lee, Y.; Gokulrangan, G.; Meyerhoff, M. E.; Wilson, G. S. *J. Biomed. Mater. Res. A* **2005**, *75*, 755−766.
(31) Finnerty, N. J.; Bolger, F. B.; Pålsson, E.; Lowry, J. P. *ACS Chem. Neurosci.* **2013**, *4*, 825−831.
(32) Kawagoe, K. T.; Wightman, R. M. *Talanta* **1994**, *41*, 865−874.
(33) Hames, D.; Hooper, N. *BIOS Instant Notes in Biochemistry*; Taylor & Francis: London, GBR, 2011.
(34) Tan, Y.; Deng, W.; Chen, C.; Xie, Q.; Lei, L.; Li, Y.; Fang, Z.; Ma, M.; Chen, J.; Yao, S. *Biosens. Bioelectron.* **2010**, *25*, 2644−2650.
(35) Du, Y.; Luo, X.-L.; Xu, J.-J.; Chen, H.-Y. *Bioelectrochemistry* **2007**, *70*, 342−347.
(36) Venton, B. J.; Michael, D. J.; Wightman, R. M. *J. Neurochem.* **2003**, *84*, 373−381.
(37) Krajewska, B. *Enzyme Microb. Technol.* **2004**, *35*, 126−139.
(38) Sanchez-Pozo, A.; Alados, J. C.; Sanchez-Medina, F. *Gen. Pharmacol.* **1988**, *19*, 281−284.
(39) Rice, M. E. *Neuroscientist* **2011**, *17*, 389−406.
(40) Spanos, M.; Gras-Najjar, J.; Letchworth, J. M.; Sanford, A. L.; Toups, J. V.; Sombers, L. A. *ACS Chem. Neurosci.* **2013**, *4*, 782−789.
(41) Fellows, L. K.; Boutelle, M. G.; Fillenz, M. *J. Neurochem.* **1992**, *59*, 2141−2147.
(42) Duarte, J. M. N.; Gruetter, R. *J. Neurochem.* **2012**, *121*, 396−406.
(43) Kikuchi, M.; Hirosawa, T.; Yokokura, M.; Yagi, S.; Mori, N.; Yoshikawa, E.; Yoshihara, Y.; Sugihara, G.; Takebayashi, K.; Iwata, Y.; Suzuki, K.; Nakamura, K.; Ueki, T.; Minabe, Y.; Ouchi, Y. *J. Neurosci.* **2011**, *31*, 11193−11199.
(44) Convit, A.; Wolf, O. T.; Tarshish, C.; de Leon, M. J. *Proc. Natl. Acad. Sci. U. S. A.* **2003**, *100*, 2019−2022.
(45) Pellerin, L.; Magistretti, P. J. *Proc. Natl. Acad. Sci. U. S. A.* **1994**, *91*, 10625−10629.
(46) Hall, C. N.; Klein-Flugge, M. C.; Howarth, C.; Attwell, D. *J. Neurosci.* **2012**, *32*, 8940−8951.
(47) Lowry, J. P.; Fillenz, M. *J. Physiol.* **1997**, *498* (Pt2), 497−501.
(48) Lowry, J. P.; O'Neill, R. D.; Boutelle, M. G.; Fillenz, M. *J. Neurochem.* **1998**, *70*, 391−396.
(49) Newman, L. A.; Korol, D. L.; Gold, P. E. *PLoS One* **2011**, *6*, e28427.